Experimental Modal Analysis Of Large Fuselage Panel For Composite Structure: Contact And Non-Contact Measurement

Marcin Luczak[1], Antonio Vecchio[1], Emiliano Mucchi[2] and Elena Pierro[3]
[1] LMS International, Interleuvenlaan 68, B-3001 Leuven, Belgium
email: marcin.luczak@lmsintl.com
email: antonio.vecchio@lms.be
[2] EnDIF-Engineering Department in Ferrara, Università degli Studi di Ferrara Via Saragat 1, I-44100 Ferrara, Italy
email: emiliano.mucchi@unife.it
[3] DIMeG-Politecnico di Bari v.le Japigia 182, 70126 Bari, Italy
email: e.pierro@poliba.it

Abstract

This paper presents the results of a research activity aimed at assessing the impact of several excitation and measure techniques used on the composite structure on the modal model parameters variability. To this aim, an intensive test campaign is carried out on an aircraft fuselage panel made of composite material. Contact and non-contact 1D and contact 3D measurements were performed. Modal models are extracted from dynamic test data collected during a test campaign on a composite material fuselage panel. Assessment of the excitation method and the measurement technique and directions on the modal model parameters is being made.

1 INTRODUCTION

Problems presented in this paper are the results of a first part of the UNVICO-2 research project oriented for testing, modelling and updating the non-deterministic FE models of the composite material structures [1]. Competitive market forces manufacturers of the composite structures to reduce the test time and depend on much less time and cost consuming numerical simulations. However computational models have to be validated against the experimental models to prove their reliability. Experimental Modal Analysis (EMA) technique is established tool for the identification of dynamic properties of structures [2-4]. Modal models can be applied in many ways, and one of them is Finite Element Method (FEM) model updating procedure [5-9]. The test data is used against the numerical simulation results to correct the parameters of the FE model as such it yields the results close to those from measurement. Second area of application of EMA could be Structural Health Monitoring (SHM) based on the observation of a value of modal parameter [10-13]. For these two applications a reliable modal test data is of vital importance. However test data is a subject of variability. Many factors such as production process, wear, material imperfections, environmental conditions on one hand and experimental setup on the other lead to scatter of a measurement data of nominally identical structures. Test data variabilities are subject of extensive studies in many research centres [14-18]. Variabilities of the test data come from number of sources. Internal source is non-repetitive production process causing that two nominally identical units have geometric and material properties within production tolerances. Example of the external source of test data variability is an environmental parameter change [19-22]. External source of test data variability could be also test setup [23, 24]. Within test setups there are three main components of the variability of measurement of the same specimen, i.e. boundary conditions, excitation method and measurement technique. Within presented research the number of experimental modal models was estimated basing on the variable test data. Change of the excitation technique and the measurement technique introduced some scatter of modal parameters. These differences are presented and assessed.

2 GOAL AND THE SCOPE OF THE INVESTIGATION

Main goal of the presented investigation is an evaluation of the influence of the excitation and measurement technique on the test data variability in modal testing of the fuselage panel. Achieving the main goal demands to go through some mid-stage tasks:

- test strategy – planning number and type of individual tests,
- planning each particular test – setup and equipment,
- carrying out the experiments,
- estimation of experimental modal models,
- comparison of the results

The panel under investigation (Figure 1) is a structure of a large area, therefore high number of measurement points should be applied. To limit mass loading phenomena caused by piezoelectric sensors applied, number of tests was carried out with a set of limited number of sensors. Random and harmonic, single and multiple excitation was applied. Contact and non-contact measurement techniques were applied to assess the sensor and wiring influence on the acquired test data. For all the configurations, assumptions of the experimental modal analysis were monitored like reciprocity and linearity check. Measured and stored were FRF and coherence functions. Seven global modal models were estimated as a final result, and the details concerning each test course are given in the corresponding test setups.

3 OBJECT OF AN INVESTIGATION

Object of an investigation is an advanced large fuselage panel presented on Figure 1. It is composed of five vertically oriented frames and seven horizontal stiffening stingers on which a three-section skin is assembled. Each of three main subcomponents is made of Carbon Fibre Reinforced Plastics, fastened by means of glue and metal joints. Dimension of the investigated panel are: Height ≈ 1700 [mm], Width ≈ 2234 [mm], Radius of the curvature ≈ 1975 [mm]. Weight of the structure is 33,25 [kg].

Figure 1 Front view of the composite fuselage panel mounted in the test rig

4 TEST RIG SETUP AND EQUIPMENT

In test campaign the following measurement and analysis tools were used:

1. Panel supported by a 3 rubber cords for providing free-free boundary condition,
2. 1 or 2 electromagnetic shakers, amplifiers, with impedance heads incorporating acceleration and force sensor in the same housing to measure driving point FRF's – Figure 2,
3. 1 or 2 triaxial modal piezoelectric accelerometers (PCB),
4. 54 or 45 uniaxial modal piezoelectric accelerometers (PCB),
5. Scanning Laser Vibrometer OFV3001S Controller, OFV055/OFV303.8 Optics, OFV042 Interface
6. Microflown probes: PU-mini NT0712-44 and USP-mini UT0608-01,
7. Frontend LMS SCADAS III with 64 channels,
8. Computer with a Test.Lab acquisition and analysis suite,
9. Geometry definitions for skin and frames –Figure 3.

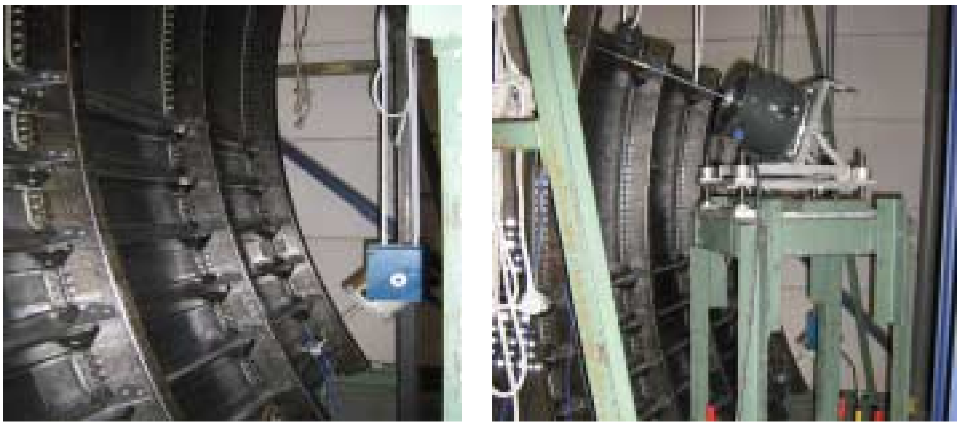

Figure 2 Shaker 1 (left) and shaker 2 (right) coupled to the panel

Measurement points were set with a distance of 0.05 [m] one from each other. Geometry definition for skin and frames is presented on left part of Figure 3. Geometry definition for the microflown probe measurement is a reduced skin geometry from piezoelectric and laser by every second row and every second column which is presented on Figure 3 on the right. Geometry for the laser and microflown measurement does not contain the frames' points.

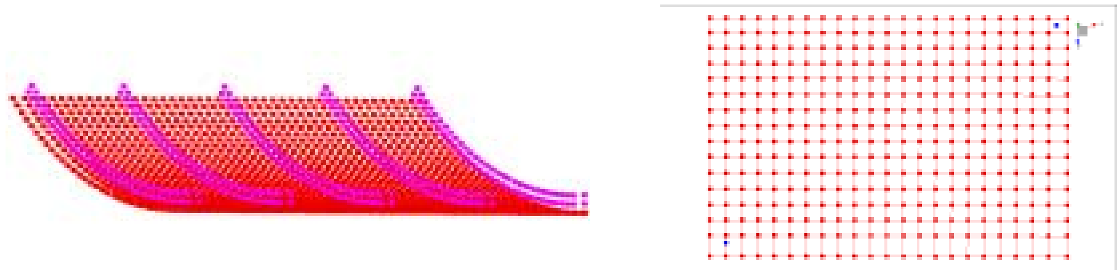

Skin (1395 points) and frames (310 points) 368 points

Figure 3 Measurement grid for skin (1395 points) and frames (310 points) for piezoelectric and laser sensors (left) and for microflown, piezoelectric reduced and laser reduced sensors (right)

5 EXPERIMENTAL MODAL ANLYSIS RESULTS

Measurement campaign was divided into three main parts: measurement with a use of piezoceramic contact accelerometers, non-contact Scanning Laser Doppler Vibrometer measurement and non contact velocity Microflown probes measurement.

5.1 Modal models from piezoelectric acceleration measurement, X and XYZ direction models.

In this subsection the six global experimental modal models estimated from contact measurement are presented. Four (M1, M2, M2R, M5) models were measured in X, out-of-plane direction only. Two models (M3, M4) were measured in all 3 directions including in-plane measurement.

MODEL 1 (M1) was estimated from 1 shaker, burst random excitation X direction measurement, 54 accelerometers and 30 sets of location of the sensors were applied to cover the skin measurement grid and 8 sets for the frames. Data from all 38 sets was analyzed in one set to obtain global modal estimates.

MODEL 2 (M2): 2 shakers burst random excitation X direction measurement, 2 impedance heads, 45 accelerometers and 35 sets of location of the sensors were applied for the skin and 8 sets for the frames. Data from all 43 sets was analyzed in one set to obtain global modal estimates. Table 1 presents examples of the mode shapes obtained for M2. For the purpose of comparison to a microflown measurement model, modal model M2R for a reduced measurement grid definition (presented on Figure 3) was estimated.

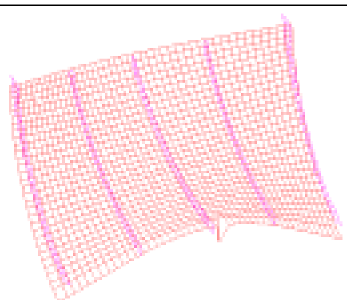	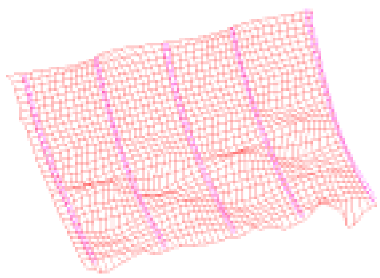
Frequency 52,4 Hz, Damping 0,89 %	Frequency 299,6 Hz, Damping 0,41 %

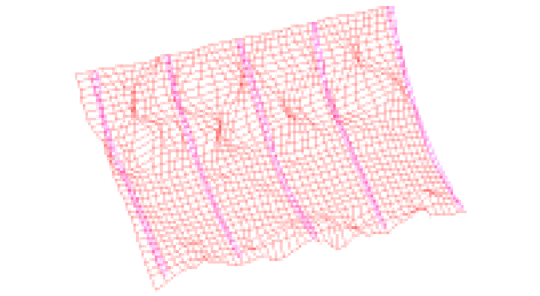	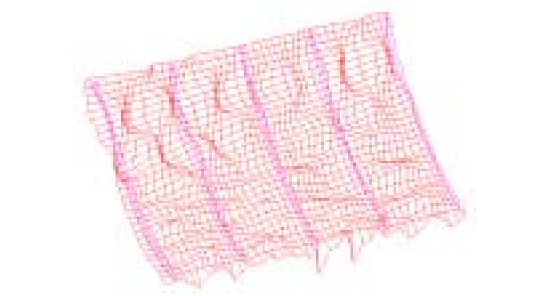
Frequency 414,8 Hz, Damping 0,36 %	Frequency 627 Hz, Damping 0,35 %

Table 1 Examples of the mode shapes for M2.

MODEL 3 (M3): setup was identical with M2. The response signal was measured also in Y and Z direction and Multi-Run modal analysis method was applied to obtain a global model. This algorithm allows merging modal models estimated for the each sensor location set to reduce mass loading effect. Runs for X Y and Z directions for both skin and frames were used to estimate 3 (set X, set Y, set Z) partial modal models. These 3 partial modal models were merged into final model.

MODEL 4 (M4) was identical with model M3 but with different shakers configuration. Runs for all 43 sets of points were analyzed individually including X Y and Z directions for both skin and frames. 43 sets were used to estimate 43 XYZ partial modal models after merged into one M4 final model. Table 2 presents examples of the mode shapes obtained for M3.

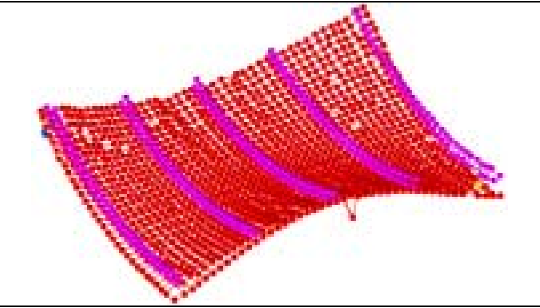	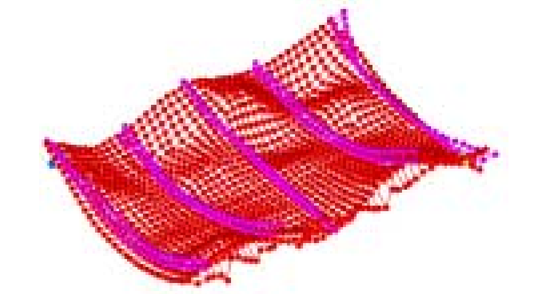
Frequency 52,8 Hz, Damping 0,53 %	Frequency 197,8 Hz, Damping 0,5 %
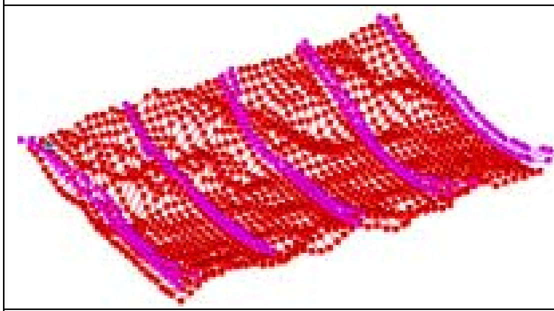	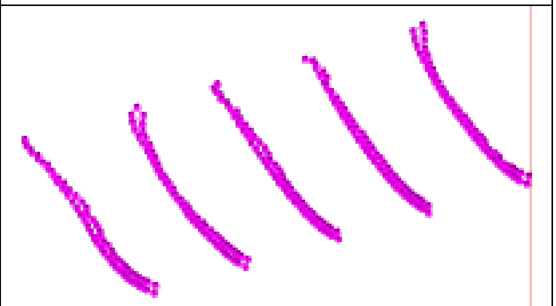
Frequency 414,9 Hz, Damping 0,27 %	Frequency 562,8 Hz, Damping 0,55 %

Table 2 Examples of the mode shapes for M3

For the XYZ models it can be observed that the transverse displacements in in-plane direction were measured for the frames.

MODEL5 (M5): 2 shakers sweep sine excitation X direction measurement, 2 impedance heads, 45 accelerometers and 35 sets of location of the sensors were applied for skin and 8 sets for the frames. Data from all 43 sets was analyzed in one set to obtain global modal estimates.

5.2 Modal models from laser measurement

For what regards the laser measurement just one model, MODEL6 (M6), has been done. In this case 2 shakers whit a burst random excitation signal, X direction measurement, 2 impedance heads, 1 Scanning Laser Vibrometer Optical Sensor and 5 sets of location of the measurement points were applied, while no measurements of the frames were performed. All runs for all 5 sets were analyzed in one set to obtain global modal estimates. Similarly to M2R modal model M6R for a reduced measurement grid definition was estimated for the purpose of comparison to a microflown. Table 3 presents examples of the mode shapes obtained for M6.

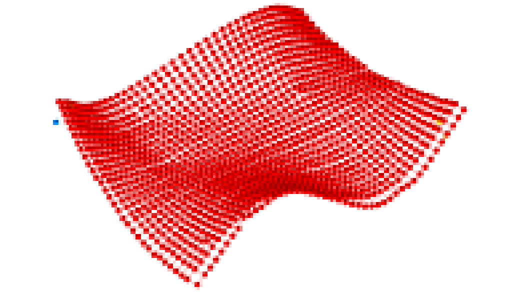	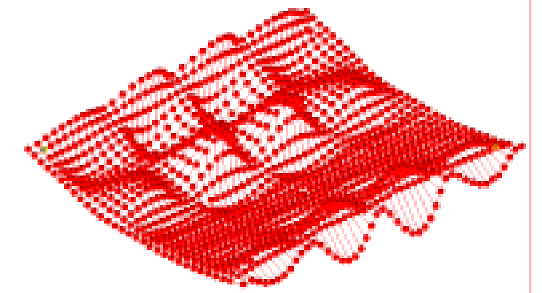
Frequency 122,6 Hz, Damping 0,43 %	Frequency 234,3 Hz, Damping 0,21 %

Table 3 Examples of the mode shapes for M6 - laser

5.3 Modal models from microflown measurement

From microflown one model, MODEL9 (M9), has been made: 2 shakers burst random excitation X direction measurement, 2 impedance heads, 2 microflown probes and 192 sets of location of the measurement points were applied for the skin, no measurements of the frames were performed. All runs for all 192 sets were analyzed in one set to obtain global modal estimates. Geometry definition for the microflown probe measurement is reduced geometry from piezoelectric and laser by every second row and every second column which is presented on Figure 3, and consists of 368 points. Table 4 presents examples of the mode shapes obtained for M9.

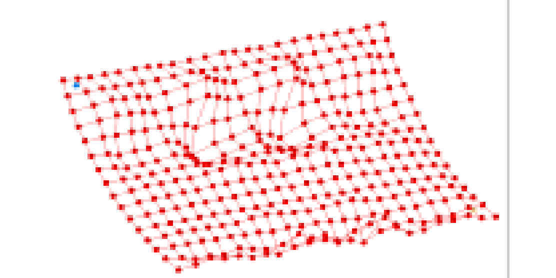	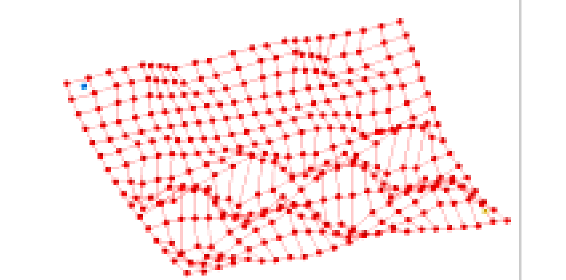
Frequency 234,317 Hz, Damping 0,351 %	Frequency 301,521 Hz, Damping 0,506 %

Table 4 Examples of the mode shapes for M9- microflowns

5.4 Modal models from piezoelectric and laser measurement

Besides the models obtained from each measurement, two hybrid models have been derived. The first, MODEL 7 (M7). is a contact/non contact X direction measurement model. Multi-Run modal analysis method was applied to obtain a global model, and runs for 5 sets of skin points were analyzed in one set. 8 frames sets were used to estimate 1 partial modal model, then merged into final model. The second hybrid model, MODEL 8 (M8) is the same as model M7, but frame measurement used is 3D.

6 COMPARISON OF THE MODAL MODELS

Modal models estimated with different excitation and measurement methods were compared to evaluate the modal data quality. Table 5 presents the comparison of frequencies of some selected natural frequencies. Table 6 presents the MAC criterion for modal vectors.

	M1		M2		M3		M4		M5		M6		M9	
Mode	Frq, Hz	Dmp, %	Frq, Hz	Dmp, %	Frq, Hz	Dmp, %	Frq, Hz	Dmp, %	Frq, Hz	Dmp, %	Frq, Hz	Dmp, %	Frq, Hz	Dmp, %
40-100														
1	52,34	0,69	52,43	0,89	52,82	0,53	52,32	0,68	52,52	0,99	52676,00	0,69	52,71	0,74
100-250														
1	117,09	0,70	117,22	0,49	116,94	0,75	117,20	0,73	116,95	0,67	117,35	0,63	117,44	0,65
2	122,37	0,52	121,94	0,46	122,16	0,52	122,24	0,52	121,91	0,24	122,62	0,43	122,55	0,49
3	156,70	1,00	156,43	1,23	156,54	1,19	156,44	1,31	156,66	1,24	157,09	1,13	157,39	1,28
4	159,96	0,45	159,84	0,52	159,84	0,52	159,92	0,50	159,94	0,37	160,71	0,44	160,65	0,45
5	180,46	0,46	180,44	0,52	180,35	0,51	180,61	0,48	180,78	0,43	181,58	0,46	181,60	0,49
6	196,29	0,56	195,42	0,80	195,44	0,77	198,11	0,55	195,67	0,70	198,75	0,40	198,72	0,42
7	199,43	0,58	199,70	0,62	197,86	0,51	200,04	0,71	199,68	0,59	200,95	0,62	200,84	0,66
8	211,31	0,44	210,11	0,64	210,15	0,54	210,45	0,50	210,24	0,63	210,94	0,37	210,87	0,51
9	218,16	0,34	217,80	0,45	217,94	0,46	217,04	0,53	217,88	0,37	219,34	0,39	219,35	0,43
10	221,69	0,40	221,00	0,62	221,13	0,62	221,19	0,39	221,57	0,47	222,44	0,47	222,41	0,57
11	232,76	0,40	232,59	0,35	232,59	0,17	232,47	0,42	232,62	0,37	234,29	0,21	234,32	0,35
12	243,23	0,38	242,49	0,49	242,60	0,46	243,49	0,56	242,51	0,46	244,03	0,41	244,17	0,44
13	245,21	0,52	245,23	0,48	245,26	0,53	245,59	0,82	245,19	0,47	246,64	0,29	246,67	0,46

Table 5 Examples of the natural frequencies and the modal damping ratio

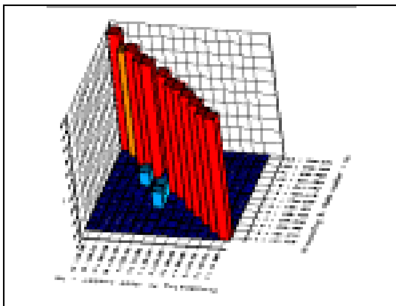	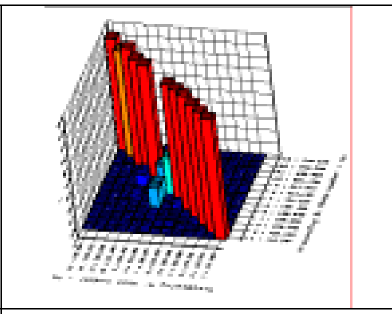	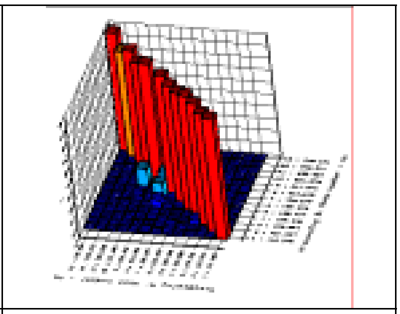
M1 ÷ M2	M1 ÷ M3	M1 ÷ M5
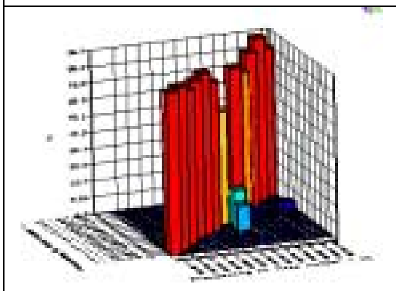	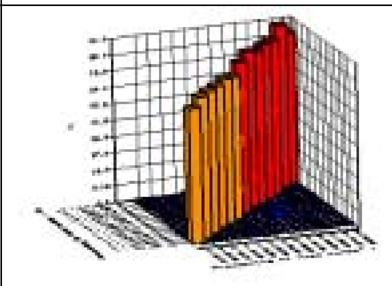	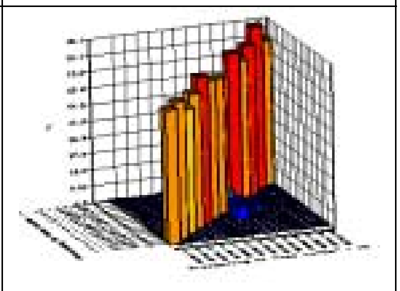
M2R ÷ M6	M6R÷M9	M2R÷M9

Table 6 Comparison of a modal models by means of MAC criterion for the frequency range 100÷250 [Hz]

Data presented in Table 5 and Table 6 clearly indicates that with increasing frequency the modal density also increases.

Other comparison method of the models is correlation analysis plotted on Figure 4.

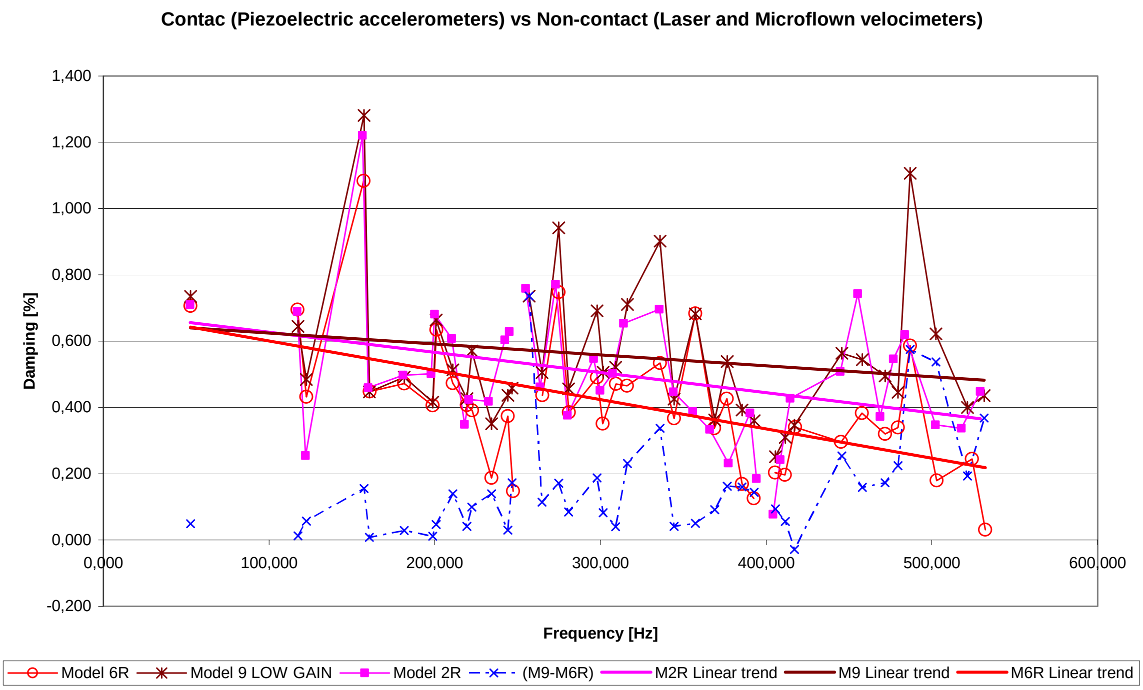

Figure 4 Assessment of the laser vibrometer, microflown probes and piezoceramic measurement on modal parameters. It is also assessment of acceleration and velocity measurement.

For contact and non-contact models the correlation chart of damping ratio and frequency is drawn. Linear trend lines are clearly demonstrating the existence of inverse correlation. Increase one of the parameters (frequency) brings decrease of the other investigated parameter (damping ratio), for all the investigated models considered. Influence of the measurement environment applied can be observed on the Figure 4. Piezoceramic sensors and their wiring system added to a measured structure results in form of mass loading effect. This effect shows up in two main ways, one is higher estimates of a damping ratio and the other one is the decrease of identified natural frequency values for the same mode towards the higher frequency range.

The new observation is from comparison of the microflown and laser measurement models. Both are non-contact techniques therefore one could expect the same order of the magnitude of estimated damping ratio for both models. This is not a case and what is more, the higher is the frequency of the mode the larger the difference becomes. For the high frequency the difference is even nearly 100% of estimated damping ratio – see (M9-M6R) curve on Figure 4. The explanation for this could be looked into the plots of measured data (Figure 5).

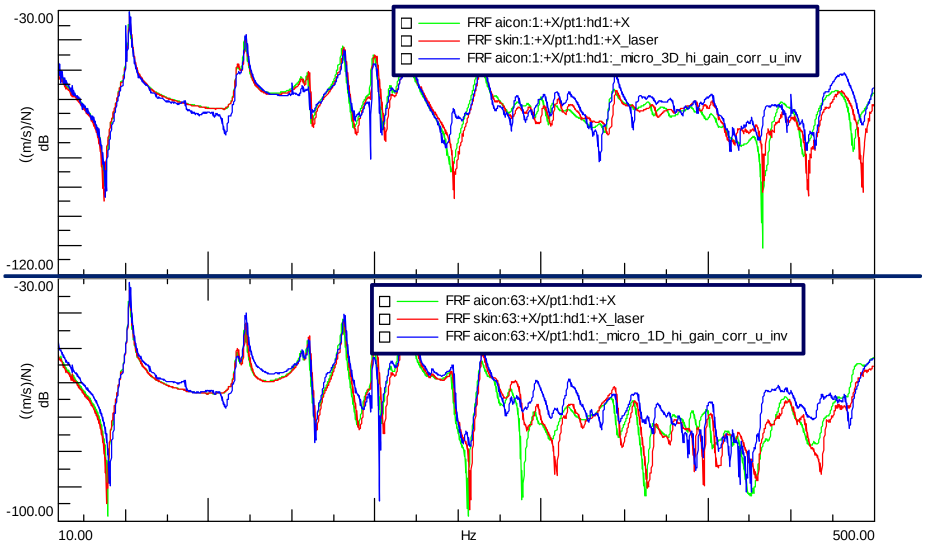

Figure 5 FRF comparison of piezoceramic, laser and microflown measurement of the same point of the panel.

The higher is the frequency the larger becomes difference in the measured FRF. This is a result of a combination of the microflown working principle and usual structure properties. It is well known that modal density of structures arises along increasing frequency values. Moreover, low frequency mode shapes are of global character, while the higher is the mode the more local mode shape becomes. Microflown probes measure the particle velocity. For the low frequencies, with relatively large displacements of a global character principle of microflown measurement is correct. With increase of frequency two factors start to contribute more to accuracy of measurement. The former is that displacements are decreasing and their amplitude is increasing. This causes the particle velocity differ more to the actual velocity of the measured surface and decreasing signal to noise ratio, as can be observed in FRF plots presented on Figure 5. The latter is that more local mode shape can introduce some interference from a particle movement of the neighboring point.

Due to curvature of a large panel skin it was difficult to maintain the constant value of the distance of a probe from a surface. Therefore this variability also contributes to a final modal model quality and especially the damping ratio. Both abovementioned reasons result in increasing differences of estimated mode shapes (see Table 3 and Table 4) and damping ratios Figure 4.

7 CONCLUSIONS

This paper presents some aspects of the multidisciplinary and interdisciplinary research oriented for the test data variability and numerical model parameters uncertainties. An extensive test campaign performed on the large composite fuselage panel was presented. Test setups included different excitation and measurement techniques of contact and non-contact type. Experimental test data examples were shown and used for modal models estimation, after compared by means of natural frequency, damping ratio and mode shapes. Some general remarks have been formulated. The common observation from displayed comparisons is that the accuracy of the results is frequency dependent. The higher the frequency of the mode becomes the larger the discrepancy between models grows.

ACKNOWLEDGEMENTS

This research was supported by Marie Curie Intra-European Fellowships within the 6th European Community Framework Programme. The authors of this work gratefully acknowledge support for this research under the project No. 038309 “UNVICO-2” provided by the EU.

REFERENCES

[1] http://cordis.europa.eu/fetch?CALLER=FP6_PROJ&ACTION=D&DOC=1&CAT=PROJ&QUERY=1198158168545&RCN=82499

[2] Uhl, T., 1997. "Komputerowo wspomagana identyfikacja modeli konstrukcji mechanicznych. Computer-aided identification of models of mechanical structures. CAD/CAM", WNT, Warszawa (in Polish)

[3] W. Heylen, S. Lammens, P. Sas, 1998 "Modal Analysis Theory and Testing", K.U. Leuven, Heverlee,

[4] Ewins, D.J., 2000, "Modal testing : theory, practice, and application," Research Studies Press, Baldock, pp. xiii, 562.

[5] Imregun, M., Visser, W. J., and Ewins, D. J., “Finite Element Model Updating using Frequency Response Function Data”, Mechanical Systems and Signal Processing, 9(2) (1995), pp. 187-202.

[6] Kwon, K., and Lin, R., “Frequency selection method for frf-based model updating”, Journal of Sound and Vibration, 278(1-2) (2004), pp. 285-306.

[7] Sinha, J. K., and Friswell, M. I., “The use of model updating for reliable finite element modelling and fault diagnosis of structural components used in nuclear plants”, Nuclear Engineering and Design, 223(1) (2003), pp. 11-23.

[8] Papadimitriou, C., Beck, J. L., and Katafygiotis, L. S., “Updating Robust Reliability using Structural Test Data”, Probabilistic Engineering Mechanics, 16(2) (2001), pp. 103-113.

[9] Mottershead, J. E., Mares, C., Friswell, M. I., “Selection and updating of parameters for an aluminium space-frame model”, Mechanical Systems and Signal Processing, 14(6) (2000), pp. 923-944.

[10] Noh, H., and Kwak, H., “Response Variability due to Randomness in Poisson’s Ratio for Plane-Strain and Plane-Stress States”, International Journal of Solids and Structures, 43(5) (2006), pp. 1093-1116.

[11] Nahvi, H., and Jabbari, M., “Crack Detection in Beams using Experimental Modal Data and Finite Element Model”, International Journal of Mechanical Sciences, 47(10) (2005), pp. 1477-1497.

[12] Garescì, F., Catalano, L., and Petrone, F., “Experimental Results of a Damage Detection Methodology using Variations in Modal Parameters”, Experimental Mechanics, 46(4) (2006), pp. 441.

[13] Macdonald, J. H. G., and Daniell, W. E., “Variation of Modal Parameters of a Cable-Stayed Bridge Identified from Ambient Vibration Measurements and FE Modelling”, Engineering Structures, 27(13) (2005), pp. 1916-1930.

[14] Deraemaeker, A., Reynders, E., De Roeck, G., “Vibration-Based Structural Health Monitoring using Output-Only Measurements Under Changing Environment”, Mechanical Systems and Signal Processing, 22(1) (2008), pp. 34-56.

[15] Sakellariou, J. S., and Fassois, S. D., “Vibration Based Fault Detection and Identification in an Aircraft Skeleton Structure Via a Stochastic Functional Model Based Method”, Mechanical Systems and Signal Processing, 22(3) (2008), pp. 557-573.

[16] Gao, W., Natural Frequency and Mode Shape Analysis of Structures with Uncertainty, Mechanical Systems and Signal Processing, 21(1) (2007), pp. 24-39.

[17] Chen, C., Duhamel, D., and Soize, C., “Probabilistic Approach for Model and Data Uncertainties and its Experimental Identification in Structural Dynamics: Case of Composite Sandwich Panels”, Journal of Sound and Vibration, 294(1-2) (2006), pp. 64-81.

[18] Capiez-Lernout, E., Pellissetti, M., Pradlwarter, H., “Data and Model Uncertainties in Complex Aerospace Engineering Systems”, Journal of Sound and Vibration, 295(3-5) (2006), pp. 923-938.

[19] Siegert D., Mevel L., Goursat M., „Experimental validation of damage monitoring techniques in variable temperature conditions“, Proceedings of IMAC XXVI A Conference and Exposition on Structural Dynamics, February 4-7 2008, Orlando, Florida, USA

[20] Xia, Y., Hao, H., Zanardo, G., Long Term Vibration Monitoring of an RC Slab: Temperature and Humidity Effect, Engineering Structures, 28(3) (2006), pp. 441-452.

[21] Ni, Y. Q., Hua, X. G., Fan, K. Q., "Correlating Modal Properties with Temperature using Long-Term Monitoring Data and Support Vector Machine Technique", Engineering Structures, 27(12) (2005), pp. 1762-1773.

[22] Sohn, S., Dzonczyk, M., Straser, E., "An Experimental Study of Temperature Effect on Modal Parameters of the Alamosa Canyon Bridge," (1999),

[23] Todd D. G., Carne T. G., "Experimental Uncertainty Quantification of Modal Test Data", Proceedings of IMAC XXV A Conference and Exposition on Structural Dynamics, February 19-22, 2007 Orlando, Florida USA

[24] Carne, T. G., Dohrmann, C. R., "Support Conditions, Their Effect on Measured Modal Parameters," Proceedings of the 16th International Modal Analysis Conference, pp. 477-483, February 1998.